

Received: 28 July 2010 – Accepted: 29 September 2010 – Published: 11 October 2010

Correspondence to: S.-C. Yoon (yoon@snu.ac.kr)

Published by Copernicus Publications on behalf of the European Geosciences Union.

ACPD

10, 23449–23495, 2010

**Simulation of the
aerosol effect on
shallow clouds over
East Asia**

I.-J. Choi et al.

Title Page

Abstract

Introduction

Conclusions

References

Tables

Figures

⏪

⏩

◀

▶

Back

Close

Full Screen / Esc

Printer-friendly Version

Interactive Discussion



Abstract

A bin-based meso-scale cloud model has been employed to explore the aerosol influence on the cloud microphysical properties and precipitation efficiency of shallow stratocumulus in East Asia in March 2005. We newly constructed aerosol size distributions and hygroscopicity parameters for five aerosol species that reproduced observed aerosol and cloud condensation nuclei (CCN) number concentrations in the target period, and thereby used in model simulation of the cloud microphysical properties and precipitation efficiency. It is found that the simulated results were satisfactorily close to the satellite-based observation. Significant effects of aerosols as well as of the meteorological condition were found in the simulated cloud properties and precipitation as confirmed by comparing maritime and polluted aerosol cases and by a sensitivity test with interchanging the aerosol conditions for two cases. Cloud droplets in the polluted condition tended to exhibit relatively narrower cloud drop spectral widths with a bias toward smaller droplet sizes than those in maritime condition, supporting the dispersion effect. The polluted aerosol condition also had a tendency of thinner and higher cloud layers than maritime aerosol condition under relatively humid meteorological condition, possibly due to enhanced updraft. In our cases, vertical structures of cloud droplet number and size were affected predominantly by the change in aerosol conditions, whereas in the structures of liquid water content and cloud fraction were influenced by both meteorological and aerosol conditions. Aerosol change made little differences in cloud liquid water, vertical cloud structure, and updraft/downdraft velocities between the maritime and polluted conditions under dry atmospheric condition. Quantitative evaluations of the sensitivity factor between aerosol and cloud parameters revealed a large sensitivity values in the target area compared to the previously reported values, indicating the strong aerosol-cloud interaction.

Simulation of the aerosol effect on shallow clouds over East Asia

I.-J. Choi et al.

Title Page

Abstract

Introduction

Conclusions

References

Tables

Figures



Back

Close

Full Screen / Esc

Printer-friendly Version

Interactive Discussion



1 Introduction

Tropospheric aerosols can alter the cloud microphysical and optical properties as well as precipitation efficiency as acting cloud condensation nuclei (CCN), thereby causing the indirect effect in the climate system. An increase in the aerosol number concentration enhances the number of cloud droplets with reduced droplet sizes for a same liquid water path, which results in an increased cloud optical depth and enhanced cloud albedo (Twomey, 1974). The reduction in cloud droplet size inhibits the precipitation efficiency (Albrecht, 1989), which furthermore induces a longer cloud lifetime and increased cloud top height with an increased liquid water path (Andreae et al., 2004; Rosenfeld et al., 2006). Both increased albedo and longer cloud lifetime exert a significant cooling effect at the Earth's surface to partially offset the warming effect caused by greenhouse gases.

These aerosol indirect effects have been regarded as one of the largest uncertainties in the current understanding of climate change. The IPCC Fourth Assessment Report (2007) concluded that the global mean radiative forcing due to the first aerosol indirect effect is approximately -0.7 W m^{-2} with substantial variation from -1.8 to -0.3 W m^{-2} at the top of the atmosphere with a low level of scientific understanding. The uncertainty regarding the aerosol indirect effects arises mainly from the poor representation of cloud microphysical processes (e.g., simplified empirical relationships or physically based parameterization) in GCMs (Lohmann and Feichter, 2005, and reference therein; Chen and Penner, 2005). Therefore, direct modeling of aerosol-cloud interaction through high resolution simulations remains of considerable importance to reduce the existing uncertainty.

Growing challenge against the difficulty in simulating aerosol indirect effects in GCMs stems from application of cloud resolving models (CRMs) to particular cloud systems (Guo et al., 2007). The CRM is the primary tool to improve the understanding of aerosol-cloud interaction with high spatial resolution, explicitly treating cloud microphysical processes and cloud-radiation interaction. Bin microphysical approach,

ACPD

10, 23449–23495, 2010

Simulation of the aerosol effect on shallow clouds over East Asia

I.-J. Choi et al.

Title Page

Abstract

Introduction

Conclusions

References

Tables

Figures

⏪

⏩

◀

▶

Back

Close

Full Screen / Esc

Printer-friendly Version

Interactive Discussion

Discussion Paper | Discussion Paper | Discussion Paper | Discussion Paper | Discussion Paper



**Simulation of the
aerosol effect on
shallow clouds over
East Asia**I.-J. Choi et al.

[Title Page](#)[Abstract](#)[Introduction](#)[Conclusions](#)[References](#)[Tables](#)[Figures](#)[Back](#)[Close](#)[Full Screen / Esc](#)[Printer-friendly Version](#)[Interactive Discussion](#)

coupled into the model of this study, provides a superior prediction of precipitation and reproduces a more realistic cloud structure than does the bulk model (Lynn et al., 2005, 2007). A key advantage of the bin-based cloud scheme is that it allows the discrete calculations of the size distributions of CCN and hydrometeors by size bins; hence it enables us to approximate the number concentration, mean/effective radius, and total volume of hydrometeors, which are important variables in the estimation of aerosol indirect effect (e.g., Khain et al., 1999). Therefore, bin-based cloud models become particularly useful when the cloud microphysics play an important role in determining cloud dynamics (e.g., feedback processes and climate projection simulation).

East Asia is one of the east coast regions of the continents where aerosol-cloud interaction is moderately active with a strong positive correlation between aerosol and cloud number (Nakajima et al., 2001). Aerosol-cloud interaction over East Asia has been investigated mainly by long-term and large-scale spatial correlations from satellite-based assessments (Sekiguchi et al., 2003; Myhre et al., 2007) or by radiation budget calculated from GCM simulations (Nakajima et al., 2003; Unger et al., 2009). A detailed analysis of the linkage between aerosol and cloud/precipitation properties in this area would be insufficient to assess the aerosol indirect effect on regional-scale climate. In particular, small-scale stratocumulus clouds with no or light precipitation, which cannot be resolved in GCMs, have a profound influence on the region-scale climate and hydrological cycle. Recent studies have examined the aerosol effect on stratocumulus clouds in relation to their significant role in the radiation budget (Jiang et al., 2006; Fan et al., 2007; Altaratz et al., 2008; Lee and Penner, 2009; Lee et al., 2009; Lu et al., 2008). Hence, a more complete understanding of aerosol-cloud interaction over shallow low-level clouds in East Asia is necessary to advance our knowledge of the regional-scale aerosol indirect effect.

The ability of any particle within an aerosol population to serve as a CCN and to nucleate cloud droplets is governed primarily by the aerosol size distribution and chemical composition as well as the supersaturation of air parcels (Pruppacher and Klett, 1997; McFiggans et al., 2006). In spite of the importance of aerosol properties, a number

of modeling studies have simplified aerosol properties with several assumptions in the calculation of aerosol indirect effect. Therefore, the aerosol size distribution, chemical composition, and detailed knowledge of how different compounds interact with water are required to accurately predict how a realistic aerosol population will experience the cloud nucleation process (Andreae and Rosenfeld, 2008; McFiggans et al., 2006).

Evidences from modeling studies, in addition, have suggested that the environmental relative humidity, temperature, and vertical wind shear are likely to be important controlling factors for cloud formation and development (Khain et al., 2005; Jiang et al., 2006; Fan et al., 2007; Lee and Penner, 2009; Lee et al., 2009). Moreover, these background meteorological conditions play a critical role in the response of cloud microphysics and precipitation by aerosol change; thus, it is difficult to accurately evaluate the aerosol effect on a cloud system without specifying the meteorological condition in which the cloud system is formed. Therefore, needed is a thorough examination of the changes in cloud/precipitation properties induced by aerosol variations under various meteorological conditions.

This study aims to improve condensation nuclei (CN; all aerosol particles upon which condensation of water vapor occurs, i.e., CN is regarded as total aerosol particles throughout this study) and CCN information (e.g., size distribution and hygroscopicity) to provide their more realistic conditions for a numerical simulation using a bin-based meso-scale non-hydrostatic model of Iguchi et al. (2008). An ultimate CRM, which should be used, may be a LES model with a grid size of less than 1 km to simulate individual shallow stratocumulus cells, but we simply used a bin-base meso-scale non-hydrostatic model with a grid size of 3 km and with a 1.5-order turbulent closure model of the Monin and Obukhov similarity theory (Saito et al., 2006). Spatial resolution of this model might be too crude to resolve each cloud cell, but Iguchi et al. (2008) confirmed that the simulated statistics of cloud microphysical parameters do not depend on the model resolution in the East China Sea region, which is also our target region, between simulations of 2 km and 7 km grid sizes. This is attributed to the fact that the target area and season tended to have a warm sea surface and relatively unstable atmospheric

Simulation of the aerosol effect on shallow clouds over East Asia

I.-J. Choi et al.

[Title Page](#)[Abstract](#)[Introduction](#)[Conclusions](#)[References](#)[Tables](#)[Figures](#)[⏪](#)[⏩](#)[◀](#)[▶](#)[Back](#)[Close](#)[Full Screen / Esc](#)[Printer-friendly Version](#)[Interactive Discussion](#)

conditions to generate a relatively larger cloud cells than those in the East Pacific region where strong atmospheric stable conditions do not permit such a crude model resolution to simulate realistic aerosol-cloud interaction (Feingold and Kreidenweis, 2002). On the other hand, we have an advantage of covering a large area to take into account the large characteristic inhomogeneity of the aerosol distribution in the target region in the spring time. Our result should be regarded as a large area statistics to be compared with that of satellite remote sensing.

Good diagnostics of the spatial distribution of CN is necessary for the reproduction of realistic cloud microphysical properties in such type of the simulation (Iguchi et al., 2008). In this regard, we focus on comparing the maritime and polluted aerosol effects on the responses of cloud microphysical properties and precipitation efficiency using realistic aerosol conditions for shallow low-level stratocumulus clouds over East Asia in March 2005. Through two case simulations with different meteorological and aerosol settings as well as two additional sensitivity simulations with interchanged aerosol condition, the following points will be addressed: (1) How different are the magnitudes in the horizontally-average of cloud/precipitation properties and the characteristics in the cloud vertical structures affected by changes in the aerosol condition under same meteorological setting? (2) Which cloud parameters are dominated by the aerosol change or by the meteorological conditions? (3) How do the variations in aerosol number influence the response of cloud/precipitation properties for the target cloud?

2 Methodology

2.1 Model description

A bin-based cloud microphysics scheme coupled with a three-dimensional non-hydrostatic dynamic model, which can treat cloud, aerosol, and radiation processes (Iguchi et al., 2008), was used in this study. The dynamic model is Non-Hydrostatic Model (NHM) developed by the Japan Meteorological Agency (Saito et al., 2006). The

Simulation of the aerosol effect on shallow clouds over East Asia

I.-J. Choi et al.

Title Page

Abstract

Introduction

Conclusions

References

Tables

Figures



Back

Close

Full Screen / Esc

Printer-friendly Version

Interactive Discussion



scheme with bin-based cloud microphysics from the Hebrew University Cloud Model (HUCM, Khain et al., 1999) was implemented into the dynamic model to replace the bulk-type cloud scheme of the NHM. In the bin-based meso-scale cloud model, a single type of water (water droplet) and six types of ice (ice crystals (plate, column and dendrite), snowflakes, graupel, and hail) are included as hydrometeors. Size distributions of these hydrometeors are distributed over 33 doubling mass bins, e.g. with a droplet radius ranging from 2 to 3251 μm . Details are described in Sect. 2 and Appendix A given by Iguchi et al. (2008). In this study, only water cloud processes (i.e., nucleation, condensation, evaporation, coalescence growth, and gravitational sedimentation) were included in the calculation for the computational limitation, excluding ice cloud microphysics.

2.2 Improvement of aerosol properties in the CCN nucleation process

The original bin-based cloud model of Iguchi et al. (2008) employed the bulk aerosol number concentrations of sulfate, sea salt, and organic carbon (OC), which are regarded as hygroscopic aerosol species, to serve as potential CCN. Aerosol size distributions were simply assumed to have one log-normal size distributions for sulfate and OC given by Takemura et al. (2002), and a power-law distribution for sea salt. Summation of the three aerosol size distributions was provided for the initial CN condition. Moreover, the aerosol chemical components of all aerosol particles were assumed to be ammonium sulfate although hygroscopicity parameter was taken care to modulate difference in the chemical components. The original model thus might produce uncertainties associated with these simplified assumptions. Consideration of both aerosol size distribution and proper chemical composition is necessary to model more realistic CCN concentration in the aerosol-CCN nucleation process. More detailed aerosol specification, therefore, should be provided for each of the five aerosol types in calculating the aerosol-CCN nucleation process of the model simulation.

Simulation of the aerosol effect on shallow clouds over East Asia

I.-J. Choi et al.

Title Page

Abstract

Introduction

Conclusions

References

Tables

Figures



Back

Close

Full Screen / Esc

Printer-friendly Version

Interactive Discussion



2.2.1 Aerosol size distribution

The aerosol size distribution of each aerosol species consists of a superposition of multi-mode lognormal distribution in this study (see Fig. 1), in contrast to the simple size distributions of the original version of the model. The adopted aerosol size distribution parameters for aerosol species are given by all three-mode log-normal forms, based on previous studies (i.e., sulfate, OC, and black carbon (BC) from Herzog et al., 2004, and references therein, and sea salt and dust particles from d'Almeida et al., 1991). To ensure that these assumed aerosol size distributions could be applied over East Asia region, we validated these size distributions with observed size-resolved mass concentrations for corresponding aerosol species from two sampling datasets by the Micro-Orifice Uniform Deposit Impactor (MOUDI). One MOUDI sampling was collected on board the NOAA R/V Ronald H. Brown from 3 to 19 April 2001 during the Aerosol Characterization Experiment (ACE)-Asia campaign (Mochida et al., 2007). The other was conducted at a ground-based measurement platform located at Gosan supersite, Jeju, Korea (33.29° N, 126.16° E), from 5 to 30 March 2005 during the Atmospheric Brown Cloud-East Asian Regional Experiment (ABC-EAREX; Nakajima et al., 2007). Although the MOUDI dataset did not cover the entire size range (approximately 0.001–10 μm) in the model calculation because of the limited cutoff size, the determined aerosol number size distributions had similar features to the observed size distributions of aerosol number concentration converted from size-segregated aerosol mass concentration during both observation periods over available size range.

2.2.2 Aerosol chemical component

Petters and Kreidenweis (2007) proposed a hygroscopicity parameter that can be used to describe the influence of chemical composition on the CCN activation of aerosol particles. This parameter (denoted as B) in the aerosol-CCN nucleation process is defined as the following (Pruppacher and Klett, 1997):

Simulation of the aerosol effect on shallow clouds over East Asia

I.-J. Choi et al.

Title Page

Abstract

Introduction

Conclusions

References

Tables

Figures

⏪

⏩

◀

▶

Back

Close

Full Screen / Esc

Printer-friendly Version

Interactive Discussion



$$B \equiv \frac{\nu\phi\varepsilon M_w \rho_{cn}}{M_{cn} \rho_w} \quad (1)$$

where ν is van't Hoff factor (the number of ions the salt disassociates into), ε is the soluble mass fraction (separating the contributions of soluble and insoluble species to the water activity and total droplet volume), Φ is the osmotic coefficient, $M_{w/cn}$ is the molecular weight of water/aerosol material, and $\rho_{w/cn}$ is the density of water/aerosol. Overall, the continental and marine aerosols were inclined into B -value ranges of 0.1–0.5 and 0.6–0.9, respectively (Pöschl et al., 2009). High variability was verified in the B -value of various aerosol chemical composition as having the range of 0.3–0.7 for sulfate (Koehler et al., 2006), 0.9–1.4 for sea salt (Koehler et al., 2006; Petters and Kreidenweis, 2007), 0.001–1.10 for dust (Koehler et al., 2009; Sullivan et al., 2009), 0.01–0.6 for organic aerosols (Rose et al., 2010; Koehler et al., 2006), and 0.01–0.3 for BC (Rose et al., 2010; Andreae and Rosenfeld, 2008). In this study, the B -value for each of the aerosol compositions, which have been widely used in aerosol modeling studies, were employed in the model calculation as proposed in Ghan et al. (2001). B -value was set to 0.51, 1.16, 0.14, 0.14, and 5×10^{-7} for sulfate, sea salt, dust, OC and BC, respectively, in the present simulations. BC aerosols were assumed to be insoluble particles in this study and therefore not to be activated into CCN, which should be modified in future improvement of the CCN calculation with realistic BC number concentration.

3 Setup of numerical experiments

Numerical simulations were conducted on 13 March (denoted as case 1) and 24 March (case 2) 2005 during the ABC-EAREX2005 in order to investigate the aerosol effect on the low-level shallow stratocumulus cloud. The simulation domain covered the East China Sea region (26–39° N, 120–132° E), centered on the west from Jeju Island, Korea. In this region, enhanced aerosol loading from various aerosol source regions

Simulation of the aerosol effect on shallow clouds over East Asia

I.-J. Choi et al.

Title Page

Abstract

Introduction

Conclusions

References

Tables

Figures

⏪

⏩

◀

▶

Back

Close

Full Screen / Esc

Printer-friendly Version

Interactive Discussion



reanalysis dataset with a horizontal resolution of $2.5^{\circ} \times 2.5^{\circ}$ and 4 times per a day, substituting for the JMA-MANAL dataset. Model calculations were performed for 12 h (from 18:00 UTC of the previous day to 06:00 UTC of the target day), and the simulation results at 03:00 UTC were primarily analyzed in this study.

Figure 2 presents the synoptic weather charts at surface level, the satellite images from the Geostationary Operational Environmental Satellite (GOES)-9 infrared channel, and the horizontal distributions of sulfate (a representative polluted continental aerosol) and sea salt (the major component of maritime aerosol) aerosol mass concentrations at the surface level from SPRINTARS simulation at the initial time on the target days. In both cases 1 and 2, strong high-pressure system was widely located over the continent and well-developed low-pressure system over the eastern part of Japan (centered on the Kuril Islands) with the frontal system. Thus, East China Sea region and Korean peninsula were influenced by the flow pattern on the edge of continental high-pressure system (mostly synoptic northerly and northwesterly winds). Low-level shallow clouds, the target of this study, appeared to exist distinctly under these northerly flows, as shown in Fig. 2b. Initial sulfate and sea salt aerosol number concentrations were obviously different between two cases (see Fig. 2c). Quantitatively, surface-level sulfate mass concentrations (with converted number concentration in parentheses) over the target cloud area were calculated to be $2.41 \pm 0.74 \mu\text{g m}^{-3}$ ($2013.5 \pm 616.96 \text{ cm}^{-3}$) and $4.57 \pm 1.60 \mu\text{g m}^{-3}$ ($3825.27 \pm 1336.62 \text{ cm}^{-3}$) for cases 1 and 2, respectively. Moreover, other anthropogenic pollutants, such as OC and BC, made noticeable different loadings (OC and BC loadings of case 2 were approximately 5.5 times and 5.2 times more than that of case 1, respectively). On the contrary, sea salt aerosol amount in case 1 ($23.99 \pm 6.99 \text{ cm}^{-3}$) was estimated to be slightly more than that of case 2 ($22.85 \pm 1.98 \text{ cm}^{-3}$). Sea salt aerosol in case 1 was more predominant than that of case 2, whereas sulfate loading of case 1 was less than that of case 2. Therefore, the aerosol loading of case 1 was characterized by a relatively maritime condition and that of case 2 by a relatively continental polluted condition.

Simulation of the aerosol effect on shallow clouds over East Asia

I.-J. Choi et al.

[Title Page](#)[Abstract](#)[Introduction](#)[Conclusions](#)[References](#)[Tables](#)[Figures](#)[⏪](#)[⏩](#)[◀](#)[▶](#)[Back](#)[Close](#)[Full Screen / Esc](#)[Printer-friendly Version](#)[Interactive Discussion](#)

Simulation of the aerosol effect on shallow clouds over East Asia

I.-J. Choi et al.

Title Page

Abstract

Introduction

Conclusions

References

Tables

Figures

⏪

⏩

◀

▶

Back

Close

Full Screen / Esc

Printer-friendly Version

Interactive Discussion

Figure 3 exhibits the initial vertical profiles of meteorological variables from the JMA-MANAL dataset and of CN number concentration from the SPRINTARS simulation for cases 1 and 2. Note that these profiles were determined by averaging the values over the area where the target clouds had been developed. Simulation domain has been characterized by a significant wind shear associated with the prevailing westerlies during the springtime. Horizontal winds in Fig. 3a,b exhibited slightly different vertical wind gradients. In case 1, vertical gradients of horizontal wind (both u - and v -components) were relatively stronger than those of case 2 (i.e. differences between the altitude of 0.93 km and 3.31 km were 18.40 and 13.38 m s^{-1} for u -wind, and 6.92 and 0.89 m s^{-1} for v -wind in cases 1 and 2, respectively). In case 1, the initial marine boundary layer, capped by a strong inversion layer, presented an almost constant potential temperature (approximately 279 K), as shown in Fig. 3c, and an increasing RH with height (up to 90.4% at about 1.5 km) in Fig. 3d. Vertical profiles of potential temperature and RH in case 2 revealed a shallower boundary layer (up to about 0.5 km) with a warmer (about 284 K) and drier (maximum RH~56.1%) air mass than that of case 1. Above the initial boundary layer in both cases, the potential temperature increased, while the RH decreased. In addition, aerosol vertical profiles, obtained from the SPRINTARS simulations, indicated a significant difference between two cases. The aerosol number concentration in the free troposphere (below 3.3 km) as well as the ground-level aerosol number in case 2 was at least twice that in case 1, influenced by the existence of upper-level anthropogenic pollutants in case 2. The most remarkable distinction between cases 1 and 2 was the considerable differences in both moisture amount and aerosol number concentration.

Another noticeable difference between two cases is the occurrence of precipitation, which was present in case 1 but not in case 2. Generally, precipitation rates due to drizzle from stratocumulus clouds are on the order of a millimeter per day or less on the ground. The 3-hourly precipitation estimates by the Tropical Rainfall Measuring Mission (TRMM) at a fine horizontal scale ($0.25^\circ \times 0.25^\circ$) (Huffman et al., 2007) confirmed a small amount of precipitation (approximately 0.25 mm/day) for case 1, averaged in

the target area, which was consistent in magnitude as well as the precipitating area from the case simulation results (described in Sect. 5). Consequently, case 1 was characterized by meteorological conditions favorable to CCN activation and cloud development (relatively strong wind shear, deeper boundary layer, and moist air condition) with primarily maritime aerosol and light precipitation, while case 2 by adverse circumstances (weak wind shear, shallow boundary layer, and dry air condition) with plenty of polluted continental aerosols and no precipitation.

4 Evaluation of model performance with the modified aerosol scheme

4.1 Calculations of CN and CCN number concentration

Using aerosol bulk number concentrations converted aerosol mass concentration from SPRINTARS simulations, CN and CCN number concentrations were calculated by newly constructed aerosol size distributions and hygroscopicity parameters in a bin-based meso-scale cloud model. Figure 4 illustrates the horizontal distributions of column-integrated CN, which is the same as the summation of aerosol number concentration of five different aerosol species, and CCN number concentrations (denoted as “this study”), compared with the differences from the original scheme with the simplified assumptions about aerosol properties (as “this study-original”) at the initial time. The horizontal distributions were found to be similar between modified column CN and CCN (at a fixed supersaturation of 0.6%) number concentrations in both cases 1 and 2. Difference caused by the modification (see “this study-original” in Fig. 4) of case 1 indicates a lower column CN number concentration (size range of $D_p > 10$ nm) over the oceanic area, but a higher CCN number concentration over the whole domain than indicated in the original scheme. This difference is due to the unrealistic power-law size distribution of sea-salt aerosol in the original scheme possibly generating too many Aitken-mode particles, exerting the higher CN number concentration. Under a given supersaturation condition, however, these small-size sea-salt aerosol particles could

Simulation of the aerosol effect on shallow clouds over East Asia

I.-J. Choi et al.

Title Page

Abstract

Introduction

Conclusions

References

Tables

Figures



Back

Close

Full Screen / Esc

Printer-friendly Version

Interactive Discussion



not be activated into CCN, thereby causing the small number of CCN over the domain region. As presented in Fig. 1c, the SPRINTARS simulations in case 2 predicted the transport of a large amount of anthropogenic pollutants (e.g., sulfate and carbonaceous aerosols) along the northwesterly winds from the industrialized region over Eastern China, which brought out the relatively higher CN and CCN number concentrations of case 2 over the target domain compared with those in case 1.

Calculated CN and CCN number concentrations at the surface level were compared with ground-based observation dataset at Gosan, Jeju during the ABC-EAREX2005 (Yum et al., 2007). The CN number concentration was continuously measured by the Condensation Particle Counter (TSI CPC-3010; $D_p > 10$ nm), and the CCN number concentration by a stream-wise thermal gradient CCN counter at a fixed supersaturation of 0.6%. Calculated CN and CCN number concentrations were provided as horizontal averages over the region of 32.5–33.5° N and 125.5–126.5° E with a size range of $D_p > 10$ nm to compare with the single-point observation dataset at Gosan. In Fig. 5a, CN number concentrations for both case 1 ($2229.1 \pm 825.3 \text{ cm}^{-3}$) and case 2 ($2944.2 \pm 1073.3 \text{ cm}^{-3}$) from the present scheme were relatively close to the observation data (3285.5 and 5103.1 cm^{-3} for cases 1 and 2, respectively), with approximately twice as many as the CN number in the original scheme. Likewise, CCN number concentrations from the present scheme, as shown in Fig. 5b, indicated the estimates ($734.4 \pm 146.9 \text{ cm}^{-3}$ and $1040.2 \pm 208.1 \text{ cm}^{-3}$ for cases 1 and 2, respectively) closer to the observed CCN (788.3 and 3247.2 cm^{-3} for cases 1 and 2, respectively) and higher CCN number concentration (by about 3.5 and 1.6 times for case 1 and 2, respectively) as compared with the original ones. However, there was still a gap between calculated and observed CN and CCN concentrations, which possibly resulted from the underestimation of aerosol mass concentration by SPRINTARS simulation or instrumental error for ground-based observations.

Consequently, when more realistic aerosol size distributions and aerosol chemical components are taken into account in the aerosol-CCN nucleation process, it becomes possible to adjust the CN number concentration over the oceanic area and to calculate

Simulation of the aerosol effect on shallow clouds over East Asia

I.-J. Choi et al.

Title Page

Abstract

Introduction

Conclusions

References

Tables

Figures

⏪

⏩

◀

▶

Back

Close

Full Screen / Esc

Printer-friendly Version

Interactive Discussion



the CCN number concentration more accurately over nearly the whole domain, with values closer to those in the observation dataset compared with the original scheme.

4.2 Cloud microphysical properties

Figure 6 displays the horizontal distributions of cloud microphysical parameters (i.e., cloud droplet effective radius near cloud top (EFR), cloud liquid water path (LWP), and cloud optical depth (COD)) for cases 1 and 2 after the simulation time of 9 h (namely, at 03:00 UTC on the target days) with Terra/MODIS cloud retrievals. The EFR and COD can be explicitly calculated from the simulated number size distribution function $f(x, y, z, r)$ for each grid point by their definition, and LWP was obtained from vertical integration of the cloud droplet number concentration (CDNC) profile weighted by their mass corresponding to the simulated size distribution function as the followings:

$$\text{EFR} = \frac{\int_{r_{\min}}^{r_{\max}} r f(x, y, z, r) \pi r^2 dr}{\int_{r_{\min}}^{r_{\max}} f(x, y, z, r) \pi r^2 dr} \quad (2)$$

$$\text{COD} = Q_{\text{ext}} \int_{z=Z_b}^{z=Z_t} \int_{r_{\min}}^{r_{\max}} f(x, y, z, r) \pi r^2 dr dz \quad (3)$$

$$\text{LWP} = \frac{4\pi}{3} \int_{z=Z_b}^{z=Z_t} \int_{r_{\min}}^{r_{\max}} \rho_w r^3 f(x, y, z, r) dr dz \quad (4)$$

where r is the cloud droplet radius, and r_{\min} and r_{\max} were $2 \mu\text{m}$ and $32 \mu\text{m}$, respectively. Also, Q_{ext} is the mean scattering efficiency which was set to 2 in the present simulation, and z_t and z_b indicated the height of the top and bottom in the simulation, respectively. The density of water droplet was represented as ρ_w . Satellite-derived

Simulation of the aerosol effect on shallow clouds over East Asia

I.-J. Choi et al.

Title Page

Abstract

Introduction

Conclusions

References

Tables

Figures

◀

▶

◀

▶

Back

Close

Full Screen / Esc

Printer-friendly Version

Interactive Discussion



variables from the Terra/MODIS sensor were obtained by the algorithm of Nakajima and Nakajima (1995) and Nakajima et al. (2005). It is obvious that model simulations reproduced well the horizontal distributions of the target cloud system (low-level shallow stratocumulus) with a large number of horizontal small-scale cloud cells over the oceanic area for both cases.

Compared to the simulation results provided by the original scheme, the present scheme resulted in nearly similar features in spatial distributions for all three cloud microphysical parameters (not shown here), but with different magnitude. Increased CN and CCN number concentrations obtained by the present model led to smaller cloud droplets ($\Delta\text{EFR} \sim -4$ and $-4.4 \mu\text{m}$) and optically thicker clouds ($\Delta\text{COD} \sim +5$ and $+2.5$ for cases 1 and 2, respectively). Also, LWP in case 1 increased with higher CN and CCN number concentrations about $\Delta\text{LWP} \sim +30 \text{ g m}^{-2}$, while that in case 2 did not change substantially. Table 1 provides the comparisons of cloud microphysical parameters (EFR, LWP, and COD), averaged over the area of $125\text{--}132^\circ \text{ E}$, $28\text{--}33^\circ \text{ N}$ at 03:00 UTC on 13 March 2005 for case 1 and $125\text{--}129.5^\circ \text{ E}$, $30.8\text{--}33.2^\circ \text{ N}$ at 03:00 UTC on 24 March 2005 for case 2 from simulations with both original and modified aerosol properties, with Terra/MODIS cloud retrievals. Comparisons among the original and present schemes and satellite-based observation revealed that three cloud microphysical parameters from the present scheme had values much closer to those of the satellite retrievals compared to those from the original scheme in case 1, as consistent with the comparisons of CN and CCN number concentrations. Although LWPs in case 2 from simulations with the original and present schemes were estimated almost identically, EFR and COD from the simulation with the present scheme remained closer to the satellite retrievals. It is concluded that the modified aerosol properties contributed significantly to the improvement in the model performance, demonstrating that the cloud microphysical properties as well as aerosol/CCN number concentrations were closer to the ground-based and satellite-based observations, thereby resulting in better simulation and reliability in the analysis using the model.

Simulation of the aerosol effect on shallow clouds over East Asia

I.-J. Choi et al.

[Title Page](#)[Abstract](#)[Introduction](#)[Conclusions](#)[References](#)[Tables](#)[Figures](#)[⏪](#)[⏩](#)[◀](#)[▶](#)[Back](#)[Close](#)[Full Screen / Esc](#)[Printer-friendly Version](#)[Interactive Discussion](#)

Simulated cloud properties in cases 1 and 2 show remarkable differences from each other not only in their horizontal distributions, but in the magnitude of cloud microphysical parameters. It cannot be concluded that the changes in only aerosol size and composition (maritime and polluted air masses for cases 1 and 2, respectively) caused these differences in the cloud properties, because the background meteorological conditions were substantially dissimilar between two cases, as illustrated in Fig. 3. Therefore, it is required for us to perform other numerical experiments to examine how the cloud microphysical properties and precipitation efficiency are controlled by aerosols in the different meteorological conditions.

5 Aerosol effects on the low-level shallow stratocumulus cloud

5.1 Description of numerical experiments

Table 2 shows the summary of four numerical experiments (two real case simulations and two sensitivity experiments) to investigate the role of aerosol and meteorological conditions. Two real cases were the same as cases 1 and 2, as described in Sect. 2.3. As mentioned above, the aerosol conditions were governed predominantly by maritime and polluted aerosols for cases 1 and 2, respectively. The meteorological condition in case 1 was considered relatively favorable for cloud formation and development compared to case 2, especially with the relatively high RH. Accordingly, the two real cases were denoted by M_{humid} (maritime aerosol condition of case 1 and meteorological setting of case 1) and P_{dry} (polluted aerosol condition of case 2 and meteorological setting of case 2). Additionally, two sensitivity experiments were designed by interchanging the aerosol loadings between cases 1 and 2 to study the effect of meteorological condition. The two additional experiments were denoted by M_{dry} (maritime aerosol condition of case 1 and the meteorological setting of case 2) and P_{humid} (polluted aerosol condition of case 2 and meteorological setting of case 1). All other model configurations were identical in the sensitivity experiments except the aerosol condition.

Simulation of the aerosol effect on shallow clouds over East Asia

I.-J. Choi et al.

Title Page

Abstract

Introduction

Conclusions

References

Tables

Figures



Back

Close

Full Screen / Esc

Printer-friendly Version

Interactive Discussion



5.2 Cloud physical and microphysical properties

Figure 7a compares cloud droplet size distributions, integrated throughout the cloud layer, with a size range of 2 to 200 μm at the simulation time of 9 h after the beginning of the simulation. The peak radius of the size distributions depended upon both aerosol loading and meteorological condition; $M_{\text{humid}} \sim 8 \mu\text{m}$, P_{humid} and $M_{\text{dry}} \sim 5 \mu\text{m}$, and $P_{\text{dry}} \sim 3 \mu\text{m}$. The CDNC themselves was undoubtedly influenced by the aerosol loading rather than by the ambient meteorological condition, because the CDNC of P_{humid} and P_{dry} were calculated to be much higher than those of M_{humid} and M_{dry} . Under a same meteorological environment, polluted aerosol conditions (P_{humid} and P_{dry}) tended to produce smaller cloud droplets than in maritime aerosol conditions (M_{humid} and M_{dry}), possibly not only because enhanced aerosol loading caused smaller cloud droplets (Twomey effect), but also because the particle size of CCN activated from anthropogenic pollutants is relatively smaller than that from maritime aerosol. Temporal evolutions of the cloud droplet size distributions in the four different numerical simulations (see Fig. 7b–e) showed that the polluted aerosol conditions (P_{humid} and P_{dry}), with larger aerosol number concentration of smaller aerosol particles, contributed to the larger droplet number of smaller cloud droplet in the beginning of cloud formation of the target cloud system (simulation time: 3 h for P_{humid} and 6 h for P_{dry}). Later in simulation time, decrease in small cloud droplet number (radius < about 10 μm) and increase in large cloud droplet number became more apparent in the maritime aerosol conditions (M_{humid} and M_{dry}) than in the polluted aerosol conditions (P_{humid} and P_{dry}). In particular, more CDNC with larger size than 50 μm in M_{humid} and P_{humid} arose from the relatively large precipitating particles by precipitation occurrence. Accordingly, cloud droplets in the polluted aerosol condition tended to exhibit relatively narrower cloud drop spectral widths (the so-called dispersion effect) than those in the maritime condition, which is consistent with the results of LES simulation by Lu and Seinfeld (2006) and observational study by Lu et al. (2007). On their basis, it could be explained by suppressed drizzle at increased aerosol loadings, which results in less spectral broadening by collision and coalescence, and more spectral narrowing by droplet condensational growth.

Simulation of the aerosol effect on shallow clouds over East Asia

I.-J. Choi et al.

Title Page

Abstract

Introduction

Conclusions

References

Tables

Figures



Back

Close

Full Screen / Esc

Printer-friendly Version

Interactive Discussion



Simulation of the aerosol effect on shallow clouds over East Asia

I.-J. Choi et al.

[Title Page](#)[Abstract](#)[Introduction](#)[Conclusions](#)[References](#)[Tables](#)[Figures](#)[Back](#)[Close](#)[Full Screen / Esc](#)[Printer-friendly Version](#)[Interactive Discussion](#)

Spatial distributions of the target cloud system (i.e., the horizontal boundary of low-level shallow stratocumulus) were simulated almost similarly between M_{humid} and P_{humid} , as well as M_{dry} and P_{dry} (not shown here), which suggests that the area of cloud formation and development are determined not by the aerosol loading and properties, but by the meteorological condition. Despite of the nearly identical horizontal distributions of stratocumulus clouds, the cloud microphysical properties vary considerably with aerosol loading and composition. Figure 8 illustrates the comparisons of cloud microphysical properties (EFR, LWP, and COD) and accumulated precipitation amount (denoted by PRCP), averaged horizontally over the target area ($28\text{--}33^\circ\text{N}$, $125\text{--}132^\circ\text{E}$ for M_{humid} and P_{humid} and $30.8\text{--}33.2^\circ\text{N}$, $125\text{--}129.5^\circ\text{E}$ for M_{dry} and P_{dry}) after the simulation for 9 h. In particular, it is worthwhile to note the LWP difference (about 54.1 g m^{-2}) between M_{humid} and P_{humid} , and almost similar LWP between M_{dry} and P_{dry} . These responses of LWP by the aerosol loading were associated with the formation of precipitation. Lu et al. (2007) reported that variability in CDNC driven by the change of aerosol number concentration can bring substantial variability in precipitation characteristics, which inevitably lead to changes in the cloud LWP. The condition of P_{humid} generated 6.8 times less precipitation amount than did M_{humid} with a delayed onset of precipitation, suggesting that maritime aerosols were activated to cloud droplets to grow favorably into precipitating particles and that polluted aerosol condition suppressed the formation of precipitation (the second aerosol indirect effect), which is supported by Khain et al. (2005) and L'Ecuyer et al. (2009). Ackerman et al. (2004) suggested that the response of the cloud LWP to changes in aerosol loading is influenced by the humidity profile and is determined by a competition between moistening from decreased surface precipitation and drying from increased entrainment of overlying air. Therefore, LWP difference between M_{humid} and P_{humid} resulted from the more precipitation amount in M_{humid} , which was considered as LWP sink, with the relatively high RH, whereas constant LWPs of M_{dry} and P_{dry} were caused by little precipitation with low RH.

5.3 Vertical profiles of cloud properties and the structures of the cloud

Vertical structures of the cloud droplet number and microphysical properties over the target cloud system were compared between maritime and polluted aerosol condition under the meteorological environments of cases 1 and 2. In order to compare the maritime and polluted aerosol effects on the cloud height and its depth, we calculated the cloud top and bottom heights, and updraft/downdraft velocities with RH profiles from four experiments (see Fig. 9). Note that the grid points with cloud droplet mixing ratio over 0.01 g kg^{-1} (the threshold value for judging the cloud existence by Pawlowska and Brenguier, 2003) at two consecutive vertical levels were included in the averaging. The scale of simulated vertical velocity might be in the range of that prescribed for shallow stratocumulus clouds by Feingold (2003) and Pringle et al. (2009). Under humid meteorological condition, polluted aerosol condition (P_{humid}) made a thinner and higher cloud layer in altitude than that in maritime aerosol condition (M_{humid}). This finding could be linked to the strengthened updraft (the maximum difference between M_{humid} and P_{humid} is about -3.1 cm s^{-1}) and wider convective area with updraft about 2.2% (the grid number with a vertical velocity stronger than 0.0 cm s^{-1} divided by total grid number) near the cloud layer in P_{humid} . According to L'Ecuyer et al. (2009) and Lee and Penner (2009), polluted aerosol conditions cause more condensational heating with an increase in surface area where the condensation is occurring, which made the updraft to increase in comparison with maritime aerosol condition. More precipitating particles, in addition, could bring the cloud bottom in M_{humid} to a lower altitude than in the experiment P_{humid} . Although the cloud geometrical depth in P_{humid} appeared to be shallower, it was optically thicker (higher COD in P_{humid}) due to more number and smaller CDNC in the cloud layer, thereby resulting in potentially larger perturbation in the radiation budget. Meteorological condition of low RH made little difference not only in the cloud top/bottom height but also in the updraft/downdraft velocities between maritime and polluted aerosol conditions. Also, relatively less moisture at altitudes higher than about 1.5 km in dry meteorological condition (M_{dry} and P_{dry}) contributed to

Simulation of the aerosol effect on shallow clouds over East Asia

I.-J. Choi et al.

Title Page

Abstract

Introduction

Conclusions

References

Tables

Figures



Back

Close

Full Screen / Esc

Printer-friendly Version

Interactive Discussion



while those in cloud fraction and LWC were clearly influenced by meteorology rather than aerosol conditions.

5.4 Responses of cloud properties with variation of aerosol number concentration

5 Sensitivity tests were conducted to investigate the dependence of CDNC, cloud microphysical parameters (EFR, LWP, and COD), and accumulated precipitation amount on the change in column CN number concentration. The CN number concentration in each size bin was determined to be 0.25, 0.5, 2.0, and 4.0 times of that in four simulations (two real cases and two sensitivity experiments). CCN number concentrations are proportional to the CN number concentrations of the predicted supersaturation in these experiments as same as those of the standard run (Iguchi et al., 2008). Figure 11 compares the relationships between column CN number concentration and cloud properties over the target cloud in the four experiments. As expected, an increase of column CN number concentration resulted in distinct decreases in EFR and accumulated PRCP, as well as increases of column CDNC and COD. In particular, increasing and decreasing tendencies of cloud parameters and precipitation amount were apparent in the range of column CN number concentration less than 10^9 cm^{-2} , excluding that of column CDNC (showing a steady increasing trend regardless of the value of column CN number concentration). When the initial aerosol concentration exceeds a critical level, most of the cloud properties become less sensitive to aerosols, implying that the aerosol effect is more pronounced in relatively small aerosol number concentrations (Fan et al., 2007). The response of LWP showed different features significantly by the precipitation occurrence, identifying an increasing LWP with more column CN number concentration under the meteorological condition of case 1, but almost constant LWP in the meteorological condition of case 2.

To quantitatively assess the strength of aerosol-cloud interaction, a number of investigations have evaluated a sensitivity factor (S) regionally and globally as defined as $S = (\partial \ln X) / (\partial \ln N_a)$ based on the relationship between columnar aerosol number

Simulation of the aerosol effect on shallow clouds over East Asia

I.-J. Choi et al.

Title Page

Abstract

Introduction

Conclusions

References

Tables

Figures

⏪

⏩

◀

▶

Back

Close

Full Screen / Esc

Printer-friendly Version

Interactive Discussion



concentration and cloud parameters (Nakajima et al., 2001; Breon et al., 2002; Feingold, 2003; Sekiguchi et al., 2003; Quass et al., 2009), where N_a stands for the column-integrated CN number concentration, and X is for the cloud parameters (e.g., EFR, LWP, COD, CDNC, and PRCP). In the same way, we calculated the sensitivity factor (S) of the cloud properties with the variation of column aerosol number concentration using a linear regression to the logarithms of model output from the four numerical experiments (M_{humid} , P_{humid} , M_{dry} and P_{dry} ; see Table 4). Similar sensitivity factors in N_a -EFR and N_a -CDNC were evaluated as -0.29 to -0.35 and 0.93 to 1.17 , respectively, which means that these parameters would be more affected by the change in the aerosol number, rather than by the meteorological condition and aerosol composition. The differences in N_a -LWP sensitivity factor should be governed by the meteorological condition, as easily guessed by our discussion in the preceding sections, especially associated with the formation process of precipitation, and hence influencing the N_a -COD sensitivity factor. The value of for N_a -PRCP factor ranged from -1.12 to -2.80 for the experiment M_{humid} , and P_{humid} , respectively, whereas values from M_{dry} and P_{dry} were not relevant for comparison because of little precipitation amount. Nakajima and Schulz (2009) reviewed the values of sensitivity factors from satellite-based analysis and global model simulations and found -0.069 to -0.203 for N_a -EFR, -0.104 to 0.227 for N_a -LWP, and 0.052 to 0.262 for N_a -COD over global ocean with large spatial differences, which are considerably smaller in magnitude than the present values. Reported values should be regarded as a mean sensitivity factor averaging for various cloud types that are significantly different from each other both spatially and temporarily. This fact, therefore, suggests that a strong aerosol-cloud interaction is possible in a favorable condition of cloud formation and development in the spring season of the East China Sea.

Simulation of the aerosol effect on shallow clouds over East Asia

I.-J. Choi et al.

[Title Page](#)[Abstract](#)[Introduction](#)[Conclusions](#)[References](#)[Tables](#)[Figures](#)[⏪](#)[⏩](#)[◀](#)[▶](#)[Back](#)[Close](#)[Full Screen / Esc](#)[Printer-friendly Version](#)[Interactive Discussion](#)

6 Summary and conclusion

A bin-based meso-scale cloud model has been used to investigate the regional-scale aerosol influence on cloud microphysical properties and precipitation efficiency of shallow stratocumulus in East Asia, provided with inhomogeneous aerosol fields by SPRINTARS. This study focused on the improvement of aerosol specification (e.g., aerosol size distribution and its hygroscopicity, B) to provide more realistic aerosol conditions. Aerosol number size distributions were determined for each of five aerosol species (i.e., sulfate, sea salt, dust, OC, and BC), and all of them showed similar features with the size distributions of aerosol number concentration converted using the MOUDI dataset from field campaigns in East Asia. In addition, B -values for each of the five aerosol compositions were employed in the model calculation. Newly constructed aerosol size distributions and hygroscopicity parameters for the five aerosol species reproduced more realistic CN and CCN number concentrations, and thereby simulated cloud microphysical properties (EFR, LWP, and COD) that more closely coincide with the retrievals from satellite-based observations, which provides reliability in the analysis of this study using model simulation results.

There are some weaknesses in the consideration of aerosol conditions provided in the present simulations. In the aerosol-CCN activation process, the values of hygroscopicity parameter for different aerosol species were based on previous studies. Long-term observation dataset for aerosol hygroscopicity properties (e.g., Hygroscopic Tandem Differential Mobility Analyzer (HTDMA)) over East Asia region contributes to supply the realistic conditions for the target region. Although nesting procedure was used to provide the initial and boundary condition for aerosol input in this study, in addition, the SPRINTARS results have a spatial resolution about 111 km that is too coarse to directly apply to the present simulation using a bin-based meso-scale cloud model (3 km). Further simulations using aerosol conditions from regional-scale aerosol chemical transport models with high spatial resolution are necessary to obtain better results.

Simulation of the aerosol effect on shallow clouds over East Asia

I.-J. Choi et al.

Title Page

Abstract

Introduction

Conclusions

References

Tables

Figures



Back

Close

Full Screen / Esc

Printer-friendly Version

Interactive Discussion



Simulation of the aerosol effect on shallow clouds over East AsiaI.-J. Choi et al.

[Title Page](#)[Abstract](#)[Introduction](#)[Conclusions](#)[References](#)[Tables](#)[Figures](#)[⏪](#)[⏩](#)[◀](#)[▶](#)[Back](#)[Close](#)[Full Screen / Esc](#)[Printer-friendly Version](#)[Interactive Discussion](#)

Subsequently, we examined the maritime and polluted aerosol effects comparatively on cloud properties and accumulated precipitation through two case simulations and two additional sensitivity simulations for shallow stratocumulus clouds over East Asia. Two cases were selected in the period of ABC-EAREX2005, and sensitivity simulations were performed by interchanging the aerosol properties between the two cases in order to investigate the response of cloud properties on the variations in aerosol loading and composition under controlled meteorological background. Cloud droplets in polluted condition tended to exhibit relatively smaller and narrower cloud drop spectral widths than those in maritime condition, supporting the dispersion effect. Comparisons of the horizontally averaged cloud microphysical properties and precipitation amount enabled us to confirm the decreased EFR and enhanced COD (the first aerosol indirect effect) under meteorological settings of both cases, and to figure out precipitation suppression with pollution aerosol loading causing a larger cloud LWP (the second aerosol indirect effect) in humid condition.

Clouds in polluted aerosol condition had a tendency to have thinner and higher cloud layers than those in maritime aerosol condition under the relatively humid meteorological condition, which is possibly associated with the strengthened updraft and wider convective area with updraft velocity. Under the dry atmospheric condition, on the other hand, aerosol changes made little differences to the cloud structure and updraft/downdraft velocities between maritime and pollution aerosol conditions. Vertical structures of CDNC and EFR were induced by the change of aerosol, rather than by the meteorological conditions, whereas those in cloud fraction and LWC were clearly influenced more by the meteorological conditions than by the aerosol conditions.

Sensitivity tests were conducted to investigate the dependence of CDNC, EFR, LWP, COD, and PRCP on the change of column CN number concentration. Similar sensitivity values in N_a -EFR and N_a -CDNC in all four simulations verified that they were influenced predominantly by the change in aerosol number, but the values in N_a -LWP and N_a -COD relied on the different meteorological condition made by RH profile and precipitation occurrence. Quantitative evaluations of the sensitivity factor (S) revealed

a large sensitivity in this study compared to the previously reported values, suggesting that a strong aerosol-cloud interaction would be possible in a favorable condition of cloud formation and development in the target region.

Various responses of cloud microphysical properties and precipitation efficiency with the change in aerosol loading and composition could magnify or diminish the aerosol indirect effect on climate, which makes the evaluation of aerosol indirect effect complicated and challenging (Guo et al., 2007). Thorough investigations on these aerosol-cloud interactions with high-resolution simulation implemented by bin-based full cloud microphysics would be expected to predict the fluctuation in the radiation budget accurately.

Acknowledgement. This research was supported by the BK21 program of the School of Earth and Environmental Sciences, Seoul National University and by the Korea Meteorological Administration Research and Development Program under Grant CATER 2006-4104. We are grateful to Michihiro Mochida for providing the MOUDI dataset during ACE-ASIA field campaign. We wish to acknowledge Takashi Nakajima for offering Terra/MODIS cloud retrieval data and Toshihiko Takemura for providing SPRINTARS simulation dataset. Helpful discussions with Daisuke Goto and Yousuke Sato are acknowledged.

References

- Ackerman, A. S., Kirkpatrick, M. P., Stevens, D. E., and Toon, O. B.: The impact of humidity above stratiform clouds on indirect aerosol climate forcing, *Nature*, 432, 1014–1017, 2004.
- Albrecht, B. A.: Aerosols, cloud microphysics, and fractional cloudiness, *Science*, 245, 1227–1230, doi:10.1126/science.245.4923.1227, 1989.
- Altaratz, O., Koren, I., Reisin, T., Kostinski, A., Feingold, G., Levin, Z., and Yin, Y.: Aerosols' influence on the interplay between condensation, evaporation and rain in warm cumulus cloud, *Atmos. Chem. Phys.*, 8, 15–24, doi:10.5194/acp-8-15-2008, 2008.
- Andreae, M. O. and Rosenfeld, D.: Aerosol-cloud-precipitation interactions. Part 1. The nature and sources of cloud-active aerosols, *Earth Sci. Rev.*, 89, 13–41, 2008.
- Andreae, M. O., Rosenfeld, D., Artaxo, P., Costa, A. A., Frank, G. P., Longo, K. M., Silva-Dias, M. A. F.: Smoking rain clouds over the Amazon, *Science*, 303, 1337–1342, 2004.

Simulation of the aerosol effect on shallow clouds over East Asia

I.-J. Choi et al.

Title Page

Abstract

Introduction

Conclusions

References

Tables

Figures



Back

Close

Full Screen / Esc

Printer-friendly Version

Interactive Discussion



Simulation of the aerosol effect on shallow clouds over East Asia

I.-J. Choi et al.

[Title Page](#)
[Abstract](#)
[Introduction](#)
[Conclusions](#)
[References](#)
[Tables](#)
[Figures](#)




[Back](#)
[Close](#)
[Full Screen / Esc](#)
[Printer-friendly Version](#)
[Interactive Discussion](#)


- Bréon, F.-M., Tanré, D., and Generoso, S.: Aerosol effect on cloud droplet size monitored from satellite, *Science*, 295, 834–838, doi:10.1126/science.1066434, 2002.
- Chen, Y. and Penner, J. E.: Uncertainty analysis for estimates of the first indirect aerosol effect, *Atmos. Chem. Phys.*, 5, 2935–2948, doi:10.5194/acp-5-2935-2005, 2005.
- 5 Choi, I.-J., Kim, S.-W., Kim, J., Yoon, S.-C., Kim, M.-H., Sugimoto, N., Kondo, Y., Miyazaki, Y., Moon, K.-J., and Han, J.-S.: Characteristics of the transport and vertical structure of aerosols during ABC-EAREX2005, *Atmos. Environ.*, 42, 8513–8523, 2008.
- d’Almeida, G. A., Koepke, P., and Shettle, E. P.: *Atmospheric Aerosols: Global Climatology and Radiative Characteristics*. A Deepak Publishing, Hampton, Virginia, 561 pp., 1991.
- 10 Fan, J., Zhang, R., Li, G., Tao, W.-K., and Li, X.: Simulations of cumulus clouds using a spectral microphysics cloud-resolving model, *J. Geophys. Res.*, 112, D04201, doi:10.1029/2006JD007688, 2007.
- Feingold, G.: Modeling of the first indirect effect: analysis of measurement requirements, *Geophys. Res. Lett.*, 30(19), 1997, doi:10/1029/2003GL017967, 2003.
- 15 Feingold, G. and Kreidenweis, S. M.: Cloud processing of aerosol as modeled by a large eddy simulation with coupled microphysics and aqueous chemistry, *J. Geophys. Res.*, 107(D23), 4687, doi:10.1029/2002JD002054, 2002.
- Ghan, S., Laulainen, N., Easter, R., Wagener, R., Nemesure, S., Champman, E., Zhang, W., and Leung, R.: Evaluation of aerosol direct radiative forcing in MIRAGE, *J. Geophys. Res.*, 20 106, 5295–5316, 2001.
- Guo, H., Penner, J. E., Herzog, M., and Pawlowska, H.: Examination of the aerosol indirect effect under contrasting environments during the ACE-2 experiment, *Atmos. Chem. Phys.*, 7, 535–548, doi:10.5194/acp-7-535-2007, 2007.
- Herzog, M., Weisenstein, D. K., and Penner, J. E.: A dynamic aerosol module for global chemical transport models: model description, *J. Geophys. Res.*, 25 109, D18202, doi:10.1029/2003JD004405, 2004.
- Huffman, G. J., Adler, R. F., Bolvin, D. T., Gu, G., Nelkin, E. J., Bowman, K. P., Stocker, E. F., and Wolff, D. B.: The TRMM multi-satellite precipitation analysis: quasi-global, multi-year, combined-sensor precipitation estimates at fine scale, *J. Hydrometeorol.*, 8, 33–55, 2007.
- 30 Iguchi, T., Nakajima, T., Khain, A. P., Saito, K., Takemura, T., and Suzuki, K.: Modeling the influence of aerosols on cloud microphysical properties in the East Asia region using a mesoscale model coupled with a bin-based cloud microphysics scheme, *J. Geophys. Res.*, 113, doi:10.1029/2007JD009774, 2008.

Simulation of the aerosol effect on shallow clouds over East Asia

I.-J. Choi et al.

[Title Page](#)
[Abstract](#)
[Introduction](#)
[Conclusions](#)
[References](#)
[Tables](#)
[Figures](#)




[Back](#)
[Close](#)
[Full Screen / Esc](#)
[Printer-friendly Version](#)
[Interactive Discussion](#)

- Intergovernmental Panel on Climate Change, Climate Change 2007: The Physical Science Basis-Contribution of Working Group I to the Fourth Assessment Report of the Intergovernmental Panel on Climate Change, Cambridge Univ. Press, Cambridge, UK, 2007.
- Jiang, H., Xue, H., Teller, A., Feingold, G., and Levin, Z.: Aerosol effects on the lifetime of shallow cumulus, *Geophys. Res. Lett.*, 33, L14806, doi:10.1029/2006GL026024, 2006.
- Koehler, K. A., Kreidenweis, S. M., DeMott, P. J., Prenni, A. J., Carrico, C. M., Ervens, B., and Feingold, G.: Water activity and activation diameters from hygroscopicity data – Part II: Application to organic species, *Atmos. Chem. Phys.*, 6, 795–809, doi:10.5194/acp-6-795-2006, 2006.
- Koehler, K. A., Kreidenweis, S. M., DeMott, P. J., Petters, M. D., Prenni, A. J., and Carrico, C. M.: Hygroscopicity and cloud droplet activation of mineral dust aerosol, *Geophys. Res. Lett.*, 36, L08805, doi:10.1029/2009GL037348, 2009.
- Khain, A. P., Pokrovsky, A., and Sednev, I.: Some effects of cloud-aerosol interaction on cloud microphysics structure and precipitation formation: numerical experiments with a spectral microphysics cloud ensemble model, *Atmos. Res.*, 52, 195–220, 1999.
- Khain, A. P., Rosenfeld, D., and Pokrovsky, A.: Aerosol impact on the dynamics and microphysics of deep convective clouds, *Q. J. Roy. Meteor. Soc.*, 131, 2639–2663, 2005.
- Kim, S.-W., Yoon, S.-C., Kim, J., and Kim, S.-Y.: Seasonal and monthly variations of columnar aerosol optical properties over East Asia determined from multi-year MODIS, LIDAR and AERONET sun/sky radiometer measurements, *Atmos. Environ.*, 41, 1634–1651, 2007.
- L'Ecuyer, T. S., Berg, W., Haynes, J., Lebsock, M., and Takemura, T.: Global observations of aerosol impacts on precipitation occurrence in warm maritime clouds, *J. Geophys. Res.*, 114, D09211, doi:10.1029/2008JD011273, 2009.
- Lee, S. S. and Penner, J. E.: Impact of solar radiation on aerosol-cloud interactions in thin stratocumulus clouds, *Atmos. Chem. Phys. Discuss.*, 9, 23791–23833, doi:10.5194/acpd-9-23791-2009, 2009.
- Lee, S. S., Penner, J. E., and Saleeby, S. M.: Aerosol effects on liquid-water path of thin stratocumulus clouds, *J. Geophys. Res.*, 114, D07204, doi:10.1029/2008JD010513, 2009.
- Lohmann, U. and Feichter, J.: Global indirect aerosol effects: a review, *Atmos. Chem. Phys.*, 5, 715–737, doi:10.5194/acp-5-715-2005, 2005.
- Lu, M.-L. and Seinfeld, J. H.: Effect of aerosol number concentration on cloud droplet dispersion: a large-eddy simulation study and implications for aerosol indirect forcing, *J. Geophys. Res.*, 111, D02207, doi:10.1029/2005JD006419, 2006.

Simulation of the aerosol effect on shallow clouds over East Asia

I.-J. Choi et al.

[Title Page](#)
[Abstract](#)
[Introduction](#)
[Conclusions](#)
[References](#)
[Tables](#)
[Figures](#)




[Back](#)
[Close](#)
[Full Screen / Esc](#)
[Printer-friendly Version](#)
[Interactive Discussion](#)


- Lu, M.-L., Conant, W. C., Jonsson, H. H., Varutbangkul, V., Flagan, R. C., and Seinfeld, J. H.: The marine stratus/stratocumulus experiment (MASE): aerosol-cloud relationships in marine stratocumulus, *J. Geophys. Res.*, 112, D10209, doi:10.1029/2006JD007985, 2007.
- Lu, M.-L., Feingold, G., Jonsson, H. H., Chuang, P. Y., Gates, H., Flagan, R. C., and Seinfeld, J. H.: Aerosol-cloud relationships in continental shallow cumulus, *J. Geophys. Res.*, 113, D15201, doi:10.1029/2007JD009354, 2008.
- Lynn, B., Khain, A. P., Dudhia, J., Rosenfeld, D., Pokrovsky, A., and Seifert, A.: Spectral (bin) microphysics coupled with a mesoscale Model (MM5). Part I: model description and first results, *Mon. Weather Rev.*, 133(1), 44, doi:10.1175/MWR-2840.1, 2005.
- Lynn, B., Khain, A., Rosenfeld, D., and Woodley, W. L.: Effects of aerosols on precipitation from orographic clouds, *J. Geophys. Res.*, 112, D10225, doi:10.1029/2006JD007537, 2007.
- McFiggans, G., Artaxo, P., Baltensperger, U., Coe, H., Facchini, M. C., Feingold, G., Fuzzi, S., Gysel, M., Laaksonen, A., Lohmann, U., Mentel, T. F., Murphy, D. M., O'Dowd, C. D., Snider, J. R., and Weingartner, E.: The effect of physical and chemical aerosol properties on warm cloud droplet activation, *Atmos. Chem. Phys.*, 6, 2593–2649, doi:10.5194/acp-6-2593-2006, 2006.
- Mochida, M., Umemoto, N., Kawamura, K., Lim, H.-J., and Turpin, B. J.: Bimodal size distributions of various organic acids and fatty acids in the marine atmosphere: Influence of anthropogenic aerosols, Asian dusts, and sea spray off the coast of East Asia, *J. Geophys. Res.*, 112, D15209, doi:10.1029/2006JD007773, 2007.
- Myhre, G., Stordal, F., Johnsrud, M., Kaufman, Y. J., Rosenfeld, D., Storelvmo, T., Kristjansson, J. E., Berntsen, T. K., Myhre, A., and Isaksen, I. S. A.: Aerosol-cloud interaction inferred from MODIS satellite data and global aerosol models, *Atmos. Chem. Phys.*, 7, 3081–3101, doi:10.5194/acp-7-3081-2007, 2007.
- Nakajima, T., Higurashi, A., Kawamoto, K., and Penner, J. E.: A possible correlation between satellite-derived cloud and aerosol microphysical parameters, *Geophys. Res. Lett.*, 28, 1171–1174, 2001.
- Nakajima, T. and Schulz, M.: What do we know about large-scale changes of aerosols, clouds, and the radiation budget?, in: *Clouds in the Perturbed Climate System: Their Relationship to Energy Balance, Atmospheric Dynamics, and Precipitation*, edited by: Heintzenberg, J. and Charlson, R. J. (Strüngmann Forum reports), MIT Press, Cambridge, 2009.
- Nakajima, T., Sekiguchi, M., Takemura, T., Uno, I., Higurashi, A., Kim, D., Sohn, B. J., Oh, S.-N., Nakajima, T. Y., Ohta, S., Okada, I., Takamura, T., and Kawamoto, K.: Significance of direct

Simulation of the aerosol effect on shallow clouds over East Asia

I.-J. Choi et al.

[Title Page](#)
[Abstract](#)
[Introduction](#)
[Conclusions](#)
[References](#)
[Tables](#)
[Figures](#)




[Back](#)
[Close](#)
[Full Screen / Esc](#)
[Printer-friendly Version](#)
[Interactive Discussion](#)


and indirect radiative forcings of aerosols in the East China Sea region, *J. Geophys. Res.*, 108, 8658, doi:10.1029/2002JD003261, 2003.

Nakajima, T., Yoon, S.-C., Ramanathan, V., Shi, G.-Y., Takemura, T., Higurashi, A., Takamura, T., Aoki, K., Sohn, B.-J., Kim, S.-W., Tsuruta, H., Sugimoto, N., Shimizu, A., Tanimoto, H., Sawa, Y., Lin, N.-H., Lee, C.-T., Goto, D., and Schutgens, N.: Overview of the ABC-EAREX2005 regional experiment and a study of the aerosol direct radiative forcing in the East Asia, *J. Geophys. Res.*, 112, D24S91, doi:10.1029/2007JD009009, 2007.

Nakajima, T. Y. and Nakajima, T.: Wide-area determination of cloud microphysical properties from NOAA AVHRR measurements for FIRE and ASTEX regions, *J. Atmos. Sci.*, 52, 4043–4059, doi:10.1175/1520-0469(1995)052<4043:WADOCM>2.0.CO;2, 1995.

Nakajima, T. Y., Uchiyama, A., Takamura, T., Tsujioka, N., Takemura, T., and Nakajima, T.: Comparisons of warm cloud properties obtained from satellite, ground, and aircraft measurements during APEX intensive observation period in 2000 and 2001, *J. Meteorol. Soc. Jpn.*, 83, 1085–1095, doi:10.2151/jmsj.83.1085, 2005.

Pawlowska, H. and Brenguier, J.-L.: An observational study of drizzle formation in stratocumulus clouds for general circulation model (GCM) parameterization, *J. Geophys. Res.*, 108(D15), 8630, doi:10.1029/2002JD002679, 2003.

Petters, M. D. and Kreidenweis, S. M.: A single parameter representation of hygroscopic growth and cloud condensation nucleus activity, *Atmos. Chem. Phys.*, 7, 1961–1971, doi:10.5194/acp-7-1961-2007, 2007.

Pöschl, U., Rose, D., and Andreae, M. O.: Climatologies of cloud-related aerosols: Part 2: particle hygroscopicity and cloud condensation nuclei activity, in: *Clouds in the Perturbed Climate System: Their Relationship to Energy Balance, Atmospheric Dynamics, and Precipitation*, edited by: Heintzenberg, J. and Charlson, R. J. (Strüngmann Forum reports), MIT Press, Cambridge, 2009.

Pringle, K. J., Carslaw, K. S., Spracklen, D. V., Mann, G. M., and Chipperfield, M. P.: The relationship between aerosol and cloud drop number concentrations in a global aerosol microphysics model, *Atmos. Chem. Phys.*, 9, 4131–4144, doi:10.5194/acp-9-4131-2009, 2009.

Pruppacher, H. R. and Klett, J. D.: *Microphysics of Clouds and Precipitation*, Kluwer Academic Publishers, 1997.

Rose, D., Nowak, A., Achtert, P., Wiedensohler, A., Hu, M., Shao, M., Zhang, Y., Andreae, M. O., and Pöschl, U.: Cloud condensation nuclei in polluted air and biomass burning smoke near the mega-city Guangzhou, China – Part 1: Size-resolved measurements and implications for

Simulation of the aerosol effect on shallow clouds over East Asia

I.-J. Choi et al.

Title Page

Abstract

Introduction

Conclusions

References

Tables

Figures

◀

▶

◀

▶

Back

Close

Full Screen / Esc

Printer-friendly Version

Interactive Discussion



the modeling of aerosol particle hygroscopicity and CCN activity, *Atmos. Chem. Phys.*, 10, 3365–3383, doi:10.5194/acp-10-3365-2010, 2010.

Rosenfeld, D., Lahav, R., Khain, A., and Pinsky, M.: Aerosol-cloud interactions control of earth radiation and latent heat release budget, *Space Sci. Rev.*, 125, 149–157, 2006.

5 Saito, K., Fujita, T., Yamada, Y., Ishida, J., Kumagai, Y., Aranami, K., Ohmori, S., Nagasawa, R., Kumagai, S., Muroi, C., Kato, T., Eito, H., and Yamazaki, Y.: The operational JMA nonhydrostatic model, *Mon. Weather Rev.*, 134, 1266, doi:10.1175/MWR3120.1, 2006.

10 Sekiguchi, M., Nakajima, T., Suzuki, K., Kawamoto, K., Higurashi, A., Rosenfeld, D., Sano, I., and Mukai, S.: A study of the direct and indirect effects of aerosols using global satellite data sets of aerosol and cloud parameters, *J. Geophys. Res.*, 108(D22), 4699, doi:10.1029/2002JD003359, 2003.

15 Sullivan, R. C., Moore, M. J. K., Petters, M. D., Kreidenweis, S. M., Roberts, G. C., and Prather, K. A.: Effect of chemical mixing state on the hygroscopicity and cloud nucleation properties of calcium mineral dust particles, *Atmos. Chem. Phys.*, 9, 3303–3316, doi:10.5194/acp-9-3303-2009, 2009.

Takemura, T., Okamoto, H., Maruyama, Y., Numaguti, A., Higurashi, A., and Nakajima, T.: Global three-dimensional simulation of aerosol optical thickness distribution of various origins, *J. Geophys. Res.*, 105(D14), 17853–17874, doi:10.1029/2000JD900265, 2000.

20 Takemura, T., Nakajima, T., Dubovik, O., Holben, B. N., and Kinne, S.: Single-scattering albedo and radiative forcing of various aerosol species with a global three-dimensional model, *J. Climate*, 15, 333–352, 2002.

Takemura, T., Nozawa, T., Emori, S., Nakajima, T. Y., and Nakajima, T.: Simulation of climate response to aerosol direct and indirect effects with aerosol transport-radiation model, *J. Geophys. Res.*, 110, D02202, doi:10.1029/2004JD005029, 2005.

25 Twomey, S.: Pollution and the planetary albedo, *Atmos. Environ.*, 8, 1251–1256, doi:10.1016/0004-6981(74)90004-3, 1974.

Unger, N., Menon, S., Koch, D. M., and Shindell, D. T.: Impacts of aerosol-cloud interactions on past and future changes in tropospheric composition, *Atmos. Chem. Phys.*, 9, 4115–4129, doi:10.5194/acp-9-4115-2009, 2009.

30 Yum, S., Roberts, G., Kim, J., Song, K., and Kim, D.: Submicron aerosol size distributions and cloud condensation nuclei concentrations measured at Gosan, Korea, during the atmospheric brown clouds-East Asian regional experiment 2005, *J. Geophys. Res.*, 112, D22S32, doi:10.1029/2006JD008212, 2007.

Simulation of the aerosol effect on shallow clouds over East Asia

I.-J. Choi et al.

Table 1. Comparisons of area-averaged cloud microphysical properties (EFR: cloud effective radius around cloud top (μm), LWP: cloud liquid water path (g m^{-2}), COD: cloud optical depth) over the target cloud region between original simulations and this study with Terra/MODIS cloud retrievals.

	Parameters	Case 1	Case 2
Original scheme	EFR	17.85±3.27	12.49±3.00
	LWP	77.87±127.23	33.65±74.55
	COD	7.43±12.86	4.21±9.09
This study	EFR	13.90±3.38	8.12±1.75
	LWP	104.60±157.58	33.93±73.98
	COD	12.85±20.18	6.73±11.29
Terra/MODIS retrievals	EFR	11.63±4.50	9.91±2.14
	LWP	110.62±112.04	85.35±55.59
	COD	18.62±62.15	15.09±22.35

[Title Page](#)
[Abstract](#)
[Introduction](#)
[Conclusions](#)
[References](#)
[Tables](#)
[Figures](#)
[Back](#)
[Close](#)
[Full Screen / Esc](#)
[Printer-friendly Version](#)
[Interactive Discussion](#)

Simulation of the aerosol effect on shallow clouds over East Asia

I.-J. Choi et al.

[Title Page](#)
[Abstract](#)
[Introduction](#)
[Conclusions](#)
[References](#)
[Tables](#)
[Figures](#)
[Back](#)
[Close](#)
[Full Screen / Esc](#)
[Printer-friendly Version](#)
[Interactive Discussion](#)

Table 2. Description of four numerical experiments (two case simulations (M_{humid} and P_{dry}), and two sensitivity experiments (M_{dry} and P_{humid}) using different aerosol condition under same meteorological background).

Experiment	Aerosol condition	Meteorological setting	Remark
M_{humid}	Case 1 (maritime)	Case 1 (humid, 13 Mar)	Case simulation
P_{humid}	Case 2 (polluted)	Case 1 (humid, 13 Mar)	Sensitivity test
M_{dry}	Case 1 (maritime)	Case 2 (dry, 24 Mar)	Sensitivity test
P_{dry}	Case 2 (polluted)	Case 2 (dry, 24 Mar)	Case simulation

Simulation of the aerosol effect on shallow clouds over East Asia

I.-J. Choi et al.

Table 3. Sensitivity values of cloud microphysical properties with respect to the increase of column aerosol number concentrations.

	M_{humid}	P_{humid}	M_{dry}	P_{dry}
N_a -EFR	-0.2949	-0.3406	-0.3367	-0.3536
N_a -LWP	0.3252	0.1876	0.0498	-0.0150
N_a -COD	0.6192	0.5101	0.3910	0.3363
N_a -CDNC	1.1775	1.0768	1.0048	0.9321
N_a -PRCP	-1.1227	-1.3115	-1.5954	-2.8024

[Title Page](#)
[Abstract](#)
[Introduction](#)
[Conclusions](#)
[References](#)
[Tables](#)
[Figures](#)
[Back](#)
[Close](#)
[Full Screen / Esc](#)
[Printer-friendly Version](#)
[Interactive Discussion](#)

Simulation of the aerosol effect on shallow clouds over East Asia

I.-J. Choi et al.

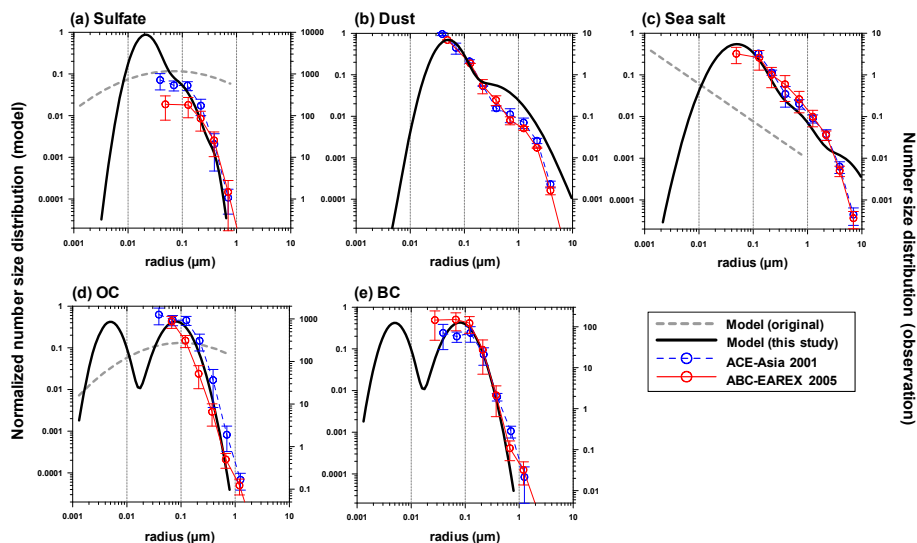


Fig. 1. Comparisons of aerosol number size distributions determined as model input (with the original distribution indicated by a thick gray dotted line and the modified distribution in this study by a thick black line) for five different aerosol species (sulfate, dust, sea salt, organic carbon, and black carbon) with those from ground-based observation during ACE-Asia in 2001 (blue circles and dotted line) and ABC-EAREX2005 (red circles and solid line). Left y-axis indicates the normalized number size distribution for model simulation, and right y-axis does the observed number size distribution.

[Title Page](#)
[Abstract](#)
[Introduction](#)
[Conclusions](#)
[References](#)
[Tables](#)
[Figures](#)
[⏪](#)
[⏩](#)
[◀](#)
[▶](#)
[Back](#)
[Close](#)
[Full Screen / Esc](#)
[Printer-friendly Version](#)
[Interactive Discussion](#)

Simulation of the aerosol effect on shallow clouds over East AsiaI.-J. Choi et al.

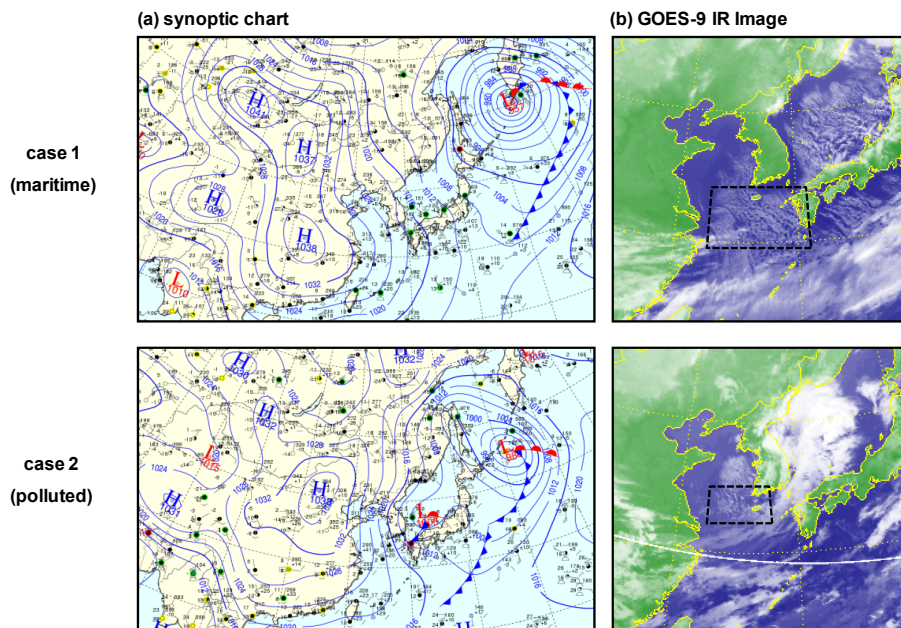
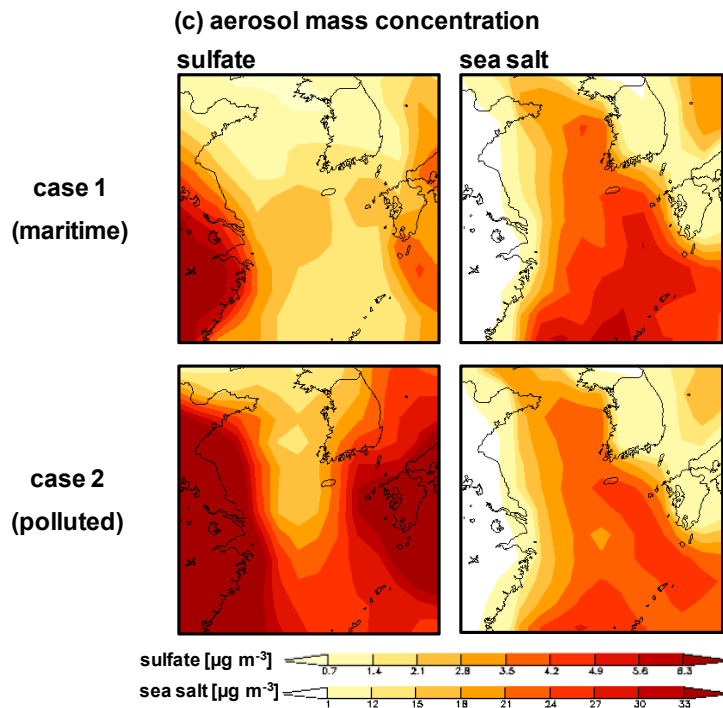


Fig. 2. Synoptic charts (surface-level) and GOES-9 IR satellite images at 00:00 UTC (<http://www.kma.go.kr>) as well as the initial mass concentrations of sulfate and sea salt aerosol (unit: $\mu\text{g m}^{-3}$) at the surface level from SPRINTARS simulations for the selected cases 1 (13 March 2005, upper panel) and 2 (24 March 2005, lower panel), respectively. Target clouds in this study are marked by dotted boxes in the satellite images.

[Title Page](#)[Abstract](#)[Introduction](#)[Conclusions](#)[References](#)[Tables](#)[Figures](#)[◀](#)[▶](#)[◀](#)[▶](#)[Back](#)[Close](#)[Full Screen / Esc](#)[Printer-friendly Version](#)[Interactive Discussion](#)

**Simulation of the
aerosol effect on
shallow clouds over
East Asia**

I.-J. Choi et al.

**Fig. 2.** Continued.[Title Page](#)[Abstract](#)[Introduction](#)[Conclusions](#)[References](#)[Tables](#)[Figures](#)[◀](#)[▶](#)[◀](#)[▶](#)[Back](#)[Close](#)[Full Screen / Esc](#)[Printer-friendly Version](#)[Interactive Discussion](#)

Simulation of the aerosol effect on shallow clouds over East Asia

I.-J. Choi et al.

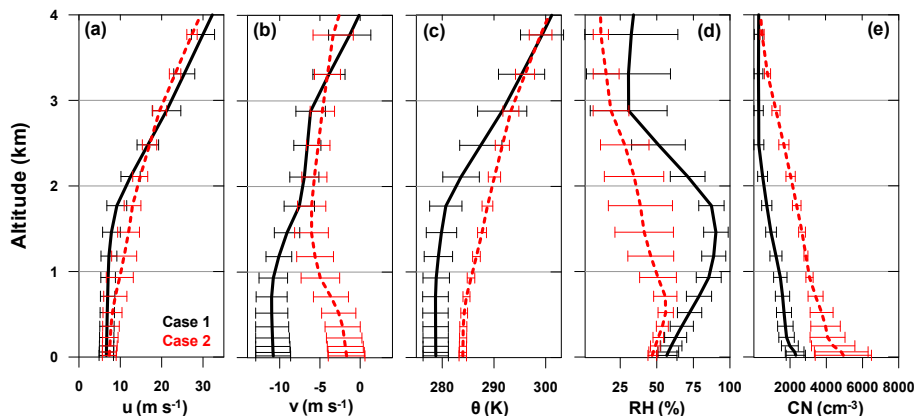


Fig. 3. Initial vertical profiles of meteorological parameters (JMA-MANAL) such as horizontal wind (**a** u -wind and **b** v -wind), (**c**) potential temperature (θ), and (**d**) relative humidity (RH) and (**e**) CN number concentration (SPRINTARS) averaged over the target area of selected cases 1 (black solid line) and 2 (red dotted line). Horizontal line indicates the standard deviation at a given altitude.

[Title Page](#)[Abstract](#)[Introduction](#)[Conclusions](#)[References](#)[Tables](#)[Figures](#)[◀](#)[▶](#)[◀](#)[▶](#)[Back](#)[Close](#)[Full Screen / Esc](#)[Printer-friendly Version](#)[Interactive Discussion](#)

Simulation of the aerosol effect on shallow clouds over East Asia

I.-J. Choi et al.

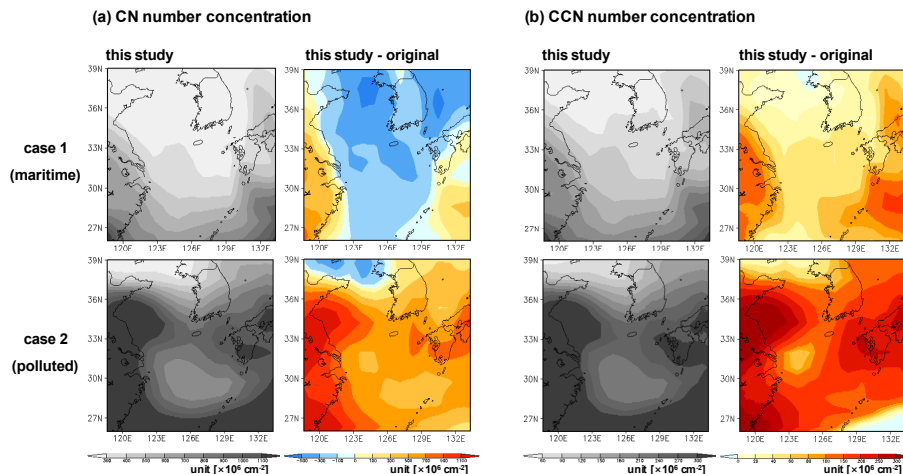


Fig. 4. Spatial distributions of vertically integrated **(a)** CN and **(b)** CCN number concentrations (unit: $\times 10^6 \text{ cm}^{-2}$) from surface to model top layer (12.45 km) from the simulation with the present aerosol scheme (this study) and the differences from the simulation with original version (this study-original) over the target model domain for cases 1 and 2.

[Title Page](#)
[Abstract](#)
[Introduction](#)
[Conclusions](#)
[References](#)
[Tables](#)
[Figures](#)
[⏪](#)
[⏩](#)
[◀](#)
[▶](#)
[Back](#)
[Close](#)
[Full Screen / Esc](#)
[Printer-friendly Version](#)
[Interactive Discussion](#)

Simulation of the aerosol effect on shallow clouds over East Asia

I.-J. Choi et al.

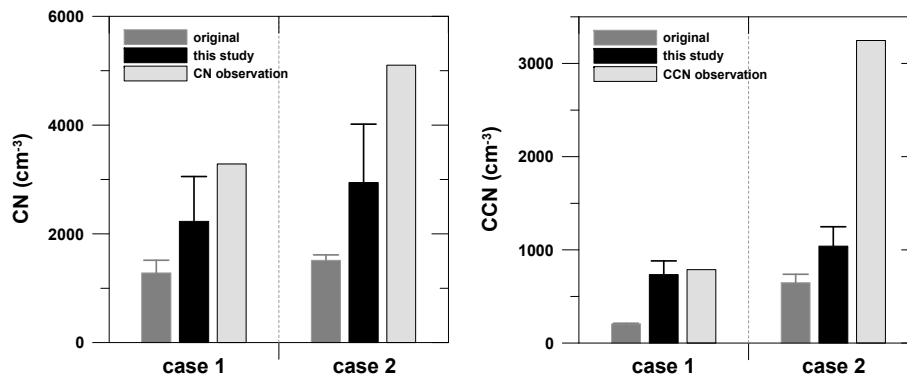


Fig. 5. Comparison between simulated CN and CCN (at 0.6% supersaturation) number concentrations at the surface level near Gosan site (averaged over the region of 125.5–126.5° E, 32.5–33.5° N) and the ground-based observation dataset at Gosan site (CN from TSI CPC3010 ($D_p > 10$ nm), CCN from CCN counter at 0.6% supersaturation).

[Title Page](#)
[Abstract](#)
[Introduction](#)
[Conclusions](#)
[References](#)
[Tables](#)
[Figures](#)
[⏪](#)
[⏩](#)
[◀](#)
[▶](#)
[Back](#)
[Close](#)
[Full Screen / Esc](#)
[Printer-friendly Version](#)
[Interactive Discussion](#)

Simulation of the aerosol effect on shallow clouds over East Asia

I.-J. Choi et al.

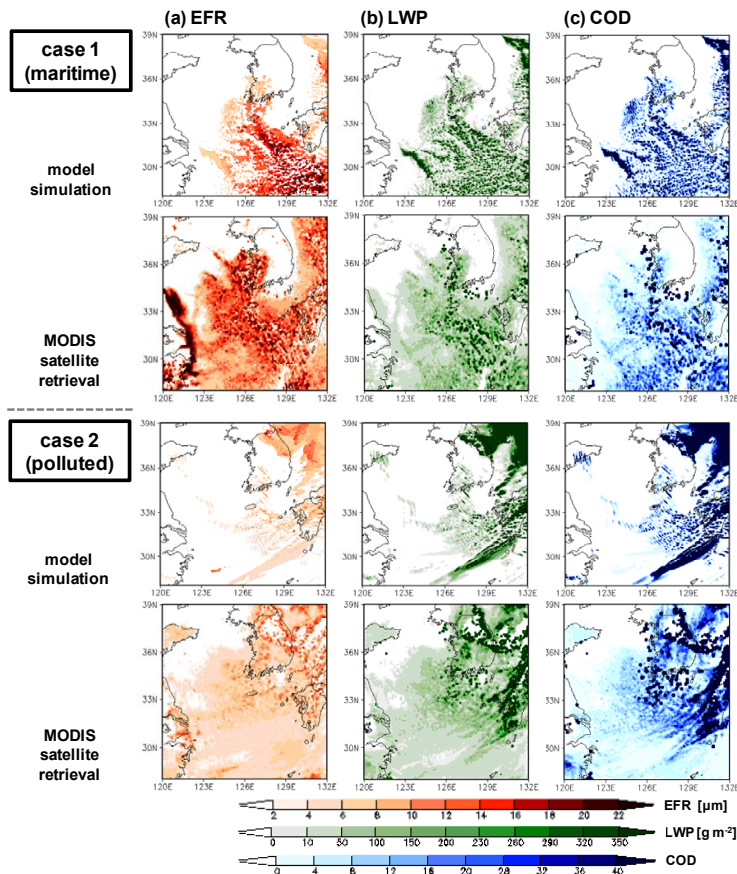


Fig. 6. Spatial distributions of (a) cloud effective radius at the cloud top (EFR, unit: μm), (b) cloud liquid water path (LWP, unit: g m^{-2}) and (c) cloud optical depth (COD, unitless) for cases 1 (two upper panels) and 2 (two lower panels), respectively, from model simulation and Terra/MODIS satellite retrievals.

[Title Page](#)
[Abstract](#)
[Introduction](#)
[Conclusions](#)
[References](#)
[Tables](#)
[Figures](#)
[⏪](#)
[⏩](#)
[◀](#)
[▶](#)
[Back](#)
[Close](#)
[Full Screen / Esc](#)
[Printer-friendly Version](#)
[Interactive Discussion](#)

Simulation of the aerosol effect on shallow clouds over East Asia

I.-J. Choi et al.

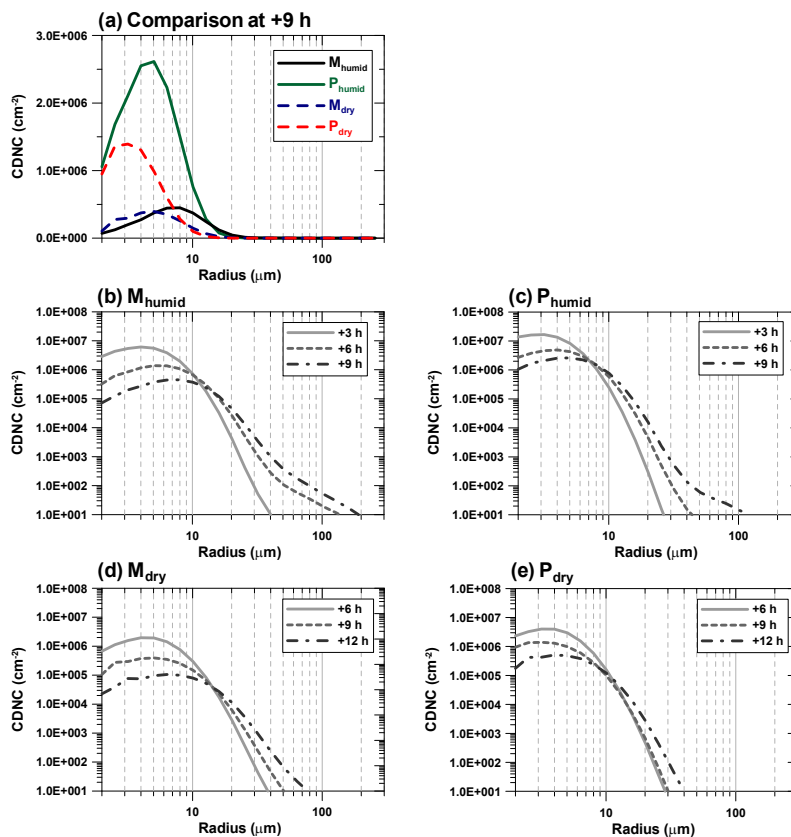


Fig. 7. (a) Size distributions of the vertically integrated cloud droplet number concentration through the cloud layer after the simulation time of 9 h from the four experiments (M_{humid} , P_{humid} , M_{dry} , and P_{dry}), and their temporal evolutions from the initial time under meteorological setting of case 1 (b and c, simulation time=3, 6, and 9 h) and case 2 (d and e, simulation time=6, 9, and 12 h). Note that the y-axis of (a) is a linear scale, and those of (b)–(e) are log scales.

[Title Page](#)
[Abstract](#)
[Introduction](#)
[Conclusions](#)
[References](#)
[Tables](#)
[Figures](#)
[⏪](#)
[⏩](#)
[◀](#)
[▶](#)
[Back](#)
[Close](#)
[Full Screen / Esc](#)
[Printer-friendly Version](#)
[Interactive Discussion](#)

Simulation of the aerosol effect on shallow clouds over East Asia

I.-J. Choi et al.

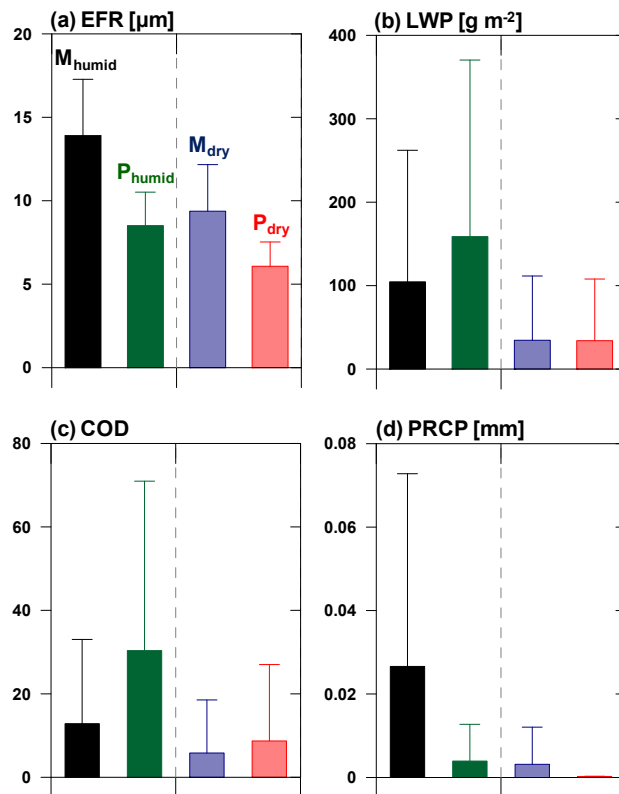


Fig. 8. Comparison of the horizontally-averaged values over the target area ($28\sim 33^{\circ}\text{N}$, $125\sim 132^{\circ}\text{E}$ for M_{humid} and P_{humid} and $30.8\sim 33.2^{\circ}\text{N}$, $125\sim 129.5^{\circ}\text{E}$ for M_{dry} and P_{dry}) at the simulation time of 9 h for cloud microphysical properties (**a** EFR, **b** LWP, and **c** COD) and (**d**) the accumulated precipitation amount (PRCP) over the target cloud region from the four numerical experiments (black: M_{humid} , green: P_{humid} , blue: M_{dry} , red: P_{dry}).

[Title Page](#)
[Abstract](#)
[Introduction](#)
[Conclusions](#)
[References](#)
[Tables](#)
[Figures](#)
[◀](#)
[▶](#)
[◀](#)
[▶](#)
[Back](#)
[Close](#)
[Full Screen / Esc](#)
[Printer-friendly Version](#)
[Interactive Discussion](#)

Simulation of the aerosol effect on shallow clouds over East Asia

I.-J. Choi et al.

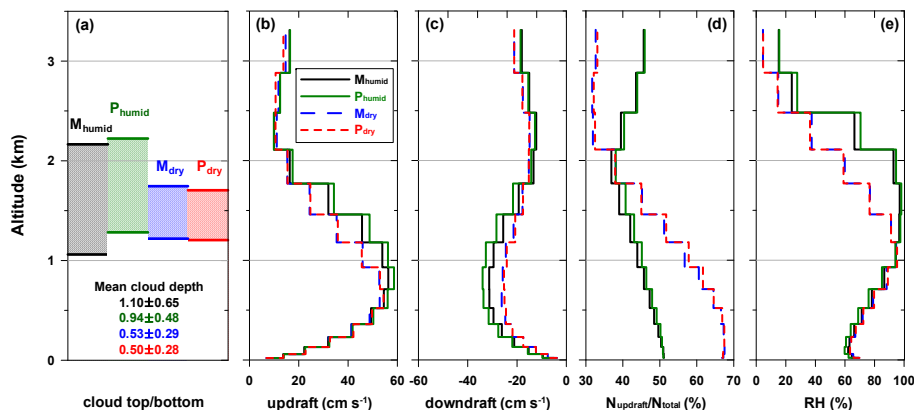


Fig. 9. Comparisons of (a) cloud top and bottom height with mean cloud depth, as well as the averaged vertical profiles of (b) updraft, (c) downdraft velocities, (d) the portion of grid with updraft velocity over target region, and (e) RH for the four experiments (black solid line: M_{humid} , green solid line: P_{humid} , blue dotted line: M_{dry} , and red dotted line: P_{dry}).

[Title Page](#)
[Abstract](#)
[Introduction](#)
[Conclusions](#)
[References](#)
[Tables](#)
[Figures](#)
[⏪](#)
[⏩](#)
[◀](#)
[▶](#)
[Back](#)
[Close](#)
[Full Screen / Esc](#)
[Printer-friendly Version](#)
[Interactive Discussion](#)

Simulation of the aerosol effect on shallow clouds over East Asia

I.-J. Choi et al.

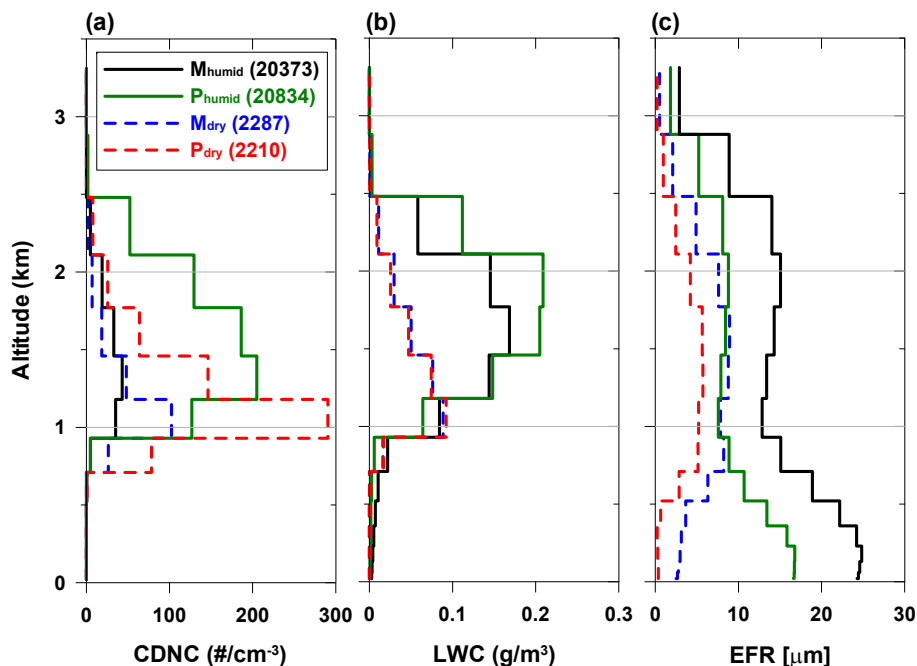


Fig. 10. Vertical profiles of (a) cloud droplet number concentration (CDNC), (b) cloud liquid water content (LWC), and (c) cloud effective radius (EFR) from four different numerical experiments. The numbers in parentheses indicate the grid number included in the averaging for each simulation.

[Title Page](#)[Abstract](#)[Introduction](#)[Conclusions](#)[References](#)[Tables](#)[Figures](#)[◀](#)[▶](#)[◀](#)[▶](#)[Back](#)[Close](#)[Full Screen / Esc](#)[Printer-friendly Version](#)[Interactive Discussion](#)

Simulation of the aerosol effect on shallow clouds over East Asia

I.-J. Choi et al.

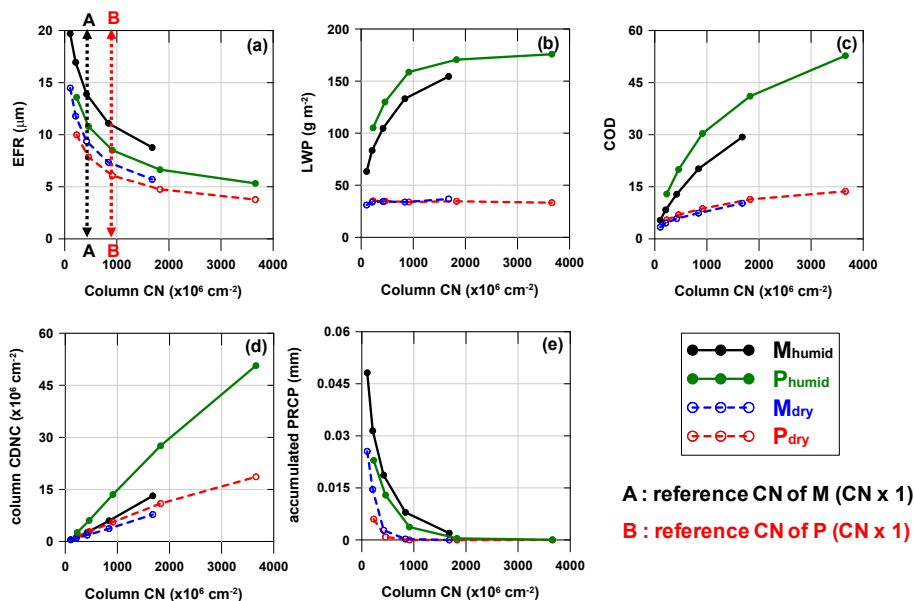


Fig. 11. Responses of cloud microphysical properties (**a** EFR, **b** LWP, **c** COD, and **d** CDNC) and accumulated precipitation amount (PRCP) by the changes of column aerosol number concentration (column CN in the x -axis) through sensitivity tests.

[Title Page](#)
[Abstract](#)
[Introduction](#)
[Conclusions](#)
[References](#)
[Tables](#)
[Figures](#)
[⏪](#)
[⏩](#)
[◀](#)
[▶](#)
[Back](#)
[Close](#)
[Full Screen / Esc](#)
[Printer-friendly Version](#)
[Interactive Discussion](#)